REVIEW ARTICLE

Fluorinated amorphous carbon films for low permittivity interlevel dielectrics

Jeremy A. Theil[a)]
ULSI Research Laboratory, Hewlett–Packard Company, Palo Alto, California 94304

(Received 23 September 1999; accepted 24 September 1999)

The need to substitute SiO_2 with low dielectric constant (κ) materials increases with each complementary metal–oxide–semiconductor process generation as interconnect RC delay, crosstalk, and power dissipation play an ever larger role in high-performance integrated circuits. Fluorinated amorphous carbon films (*a*-C:F,H) with low-κ properties ($\kappa \sim 2.0$–2.4) deposited by plasma-assisted chemical vapor deposition (CVD) techniques provide several advantages including low temperature processing, good gap fill capabilities, minimal moisture absorption, and simple implementation. Several deposition techniques have been examined, including high-density plasma and parallel-plate plasma-assisted CVD. In each case, it is possible to deposit *a*-C:F,H films with widely varying properties, such as κ and thermal stability. This has led to a good deal of confusion as to what is required to produce useful material. Results from many different sources are examined to develop a coherent picture of the relationships between deposition techniques, microstructural features, and macroscopic properties, and to summarize the scientific and technical challenges that remain for *a*-C:F,H implementation. The relationships between film deposition parameters such as applied substrate bias and film properties are presented in the discussion. In addition, x-ray photoelectron spectroscopy and network constraint theory are used to develop connections between microstructural and macroscopic properties, as well as to show how deposition parameters can be used to create a predictive model. This will demonstrate what process parameters are important in film formation. Finally, efforts to incorporate this material into integrated circuits, as well as measurements of the reliability and performance will be reviewed. [S0734-211X(99)16006-2]

I. INTRODUCTION

One side effect of downward scaling of integrated circuit components is that interconnect properties increasingly dominate circuit performance and reliability. While circuit design and layout have helped avoid these issues in the past, changes to the materials that make up the interconnect are becoming necessary. The attempts to change interconnect materials to enhance integrated circuit performance have concentrated on reducing the dielectric constant of the insulators or the resistivity of the conductors. Some performance issues where material substitution can have the greatest impact are signal propagation delay, as characterized by the RC time constant, crosstalk, power dissipation, and electromigration. With respect to lowering the dielectric constant, many materials have been examined such as fluorinated SiO_2, fluorinated amorphous carbon (*a*-C:F,H), spin-on organic films, spin-on glasses, parylenes, organo-silane/H_2O_2 chemical vapor deposition (CVD), liquid-deposited glasses, xerogels, aerogels, and phase-separated materials.[1–14] A few of these materials are already being used in manufacturing, but they tend to provide small improvements in κ. The more advanced materials ($\kappa < 3.5$), are not yet in volume production.

Of these materials, *a*-C:F,H provides intriguing characteristics from both the scientific viewpoint of why these films have such low dielectric constants, as well as the practical viewpoint of developmental cost. It has been shown that these films can achieve κ as low as 2.0, and that it appears to be controlled by composition and film density.[3] Because these are plasma-deposited films, they have an extremely high crosslink density with respect to spin-on organic films, and hence do not have a detectable glass transition temperature. They have structural similarities to hydrogenated amorphous carbon (*a*-C:H), giving them the potential to have higher thermal conductivity than SiO_2. These structural similarities may also translate to similar thermal stability and stiffness. There are also several practical reasons to examine *a*-C:F,H films for integrated circuit applications. The deposition equipment currently exists in production, and the feedstock gases tend to be nonproprietary, inexpensive, and readily available. Chemical vapor deposition (CVD) techniques, in general, have the advantage of being able to completely fill narrow features (i.e., features with a high aspect ratio, AR) better than other deposition techniques. Finally, they are also generally considered compatible with damascene process flows as well.

This article is divided into four sections. The background

a)Electronic mail: jeremy_theil@hpl.hp.com

section discusses interconnect performance issues such as signal propagation delay, power dissipation, and crosstalk from a materials point of view, as well as the different approaches to deposit *a*-C:F,H films. The results section presents data in order to characterize and understand the film formation and microstructure. The data also will be used to reveal the issues involved with integrating *a*-C:F,H films. The topics covered include electrical properties, thermal conductivity, thermal stability, adhesion, gap fill capability, and process integration. The discussion section will present a framework for understanding some of the connections between microstructural and macroscopic properties of the films using x-ray photoelectron spectroscopy (XPS) and network constraint theory. A model to predict film properties based on process parameters will be presented. It will also discuss the ramifications of reactor design on films, and the potential of chemical and thermal stability issues. Finally, the summary section will discuss unresolved issues and open questions that are still facing *a*-C:F,H films before they can be incorporated into advanced integrated circuit interconnects.

II. BACKGROUND

Signal propagation delay is the primary performance metric for high-speed complementary metal–oxide–semiconductor (CMOS) circuits, and is typically expressed as the RC delay time constant. RC delay is defined as the product of the resistance and capacitance of a circuit; these are proportional to material parameters by resistivity, ρ, of the conductor and permittivity, κ, of the insulator and geometry. Since circuit scaling generally increases RC delay, one way to mitigate it is to lower κ and/or ρ. Crosstalk can also limit circuit performance. Crosstalk is a measure of the coupling of a signal from one portion of a circuit to another. It is related to material parameters by the ratio of the intralayer capacitance ($C_{\parallel}$), over the sum of $C_{\parallel}$ and the interlayer capacitance ($C_{\perp}$).[15] Normally, crosstalk is confined to a few critical areas of the circuit, and is minimized by increasing the dielectric thickness between lines only in those critical areas. Increasing clock speeds and decreasing operating voltages now render circuits more susceptible to crosstalk, making such spatial corrections less practical. It has been shown that decreasing the intralayer capacitance relative to the interlayer capacitance can minimize crosstalk.[15,16] The implication is that intralayer material changes can benefit crosstalk without altering the circuit dimensions. From a κ point of view, this implies that using lower κ material for the intralayer dielectric relative to the interlayer dielectric can lower crosstalk. Power dissipation of CMOS circuitry is defined by $p=CV^2f$, where p is power, C is circuit capacitance, f is operating frequency, and V is operating voltage.[17,18] While there are circuit layout techniques to minimize power dissipation, only decreasing interconnect capacitance will minimize interconnect power dissipation with respect to frequency.

Simulations of circuit performance as a function of material changes that affect the RC time delay constant demonstrate the relative improvement in circuit performance. Figure 1 is a chart that compares rise time variation for different conductor metals for different line lengths. Below 2 mm, there is very little difference between lines, however, 5 mm lines show a 15% improvement between Cu and Al. In simulations of SRAM circuits, substitution of Cu for Al metallization, a 33% drop in R decreases the RC delay by 4–7%. By contrast, decreasing the κ from 4.0 to 2.5 for a 38% drop in C decreases the RC delay by 8–13%.[19] This demonstrates that a greater delay reduction is obtained by lowering C by a given fraction than by lowering R by the same fraction. The reason for this is that interconnect capacitance contributes more to total circuit capacitance than line resistance contributes to total circuit resistance. In fact, the main advantage of using copper is not to lower RC delay, but to improve electromigration reliability which in turn allows for the use of smaller wiring dimensions. In this case, optimization of dimensions is the primary factor in RC reduction.[20]

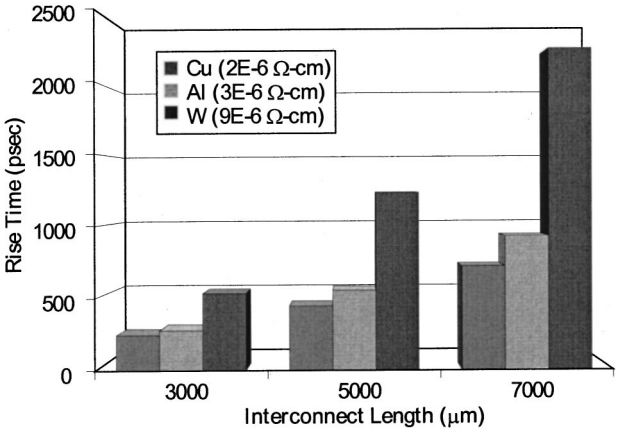

FIG. 1. Effect of interconnect metal on line rise time as a function of line length.

Most accounts of circuit delay only consider the impact of changes in interconnect material properties on the intercon-

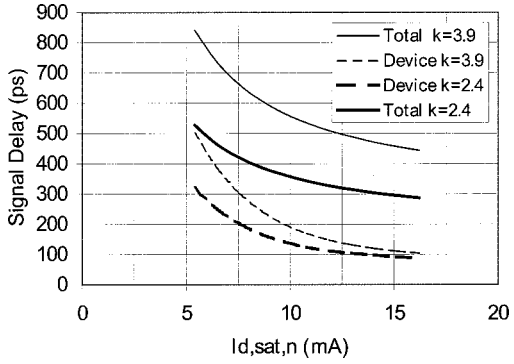

FIG. 2. Effect of $I_{d,\mathrm{sat}}$ on signal delay. FET (labeled as the Device) and total contribution to circuit delay. The difference between the two curves is the influence of the interconnect. Model assumed a 5 mm line length driven by an inverter in which all FETs are the same size. The solid lines show the total delay, while the dashed lines show the logic gate contribution. The thinner lines are for a dielectric κ=3.9, while the thicker lines are for a low-κ material with κ=2.4 (courtesy of Sam Nakagawa, Hewlett–Packard Company).

nect delay. In reality, however, changes in ρ or κ affect not only the interconnect delay but transistor-based delay phenomena as well. Figure 2 is a plot of a simulation that illustrates the contribution of field effect transistor (FET) and interconnect and their interactions as the dielectric constant of the insulator is reduced. There are three features of this plot that demonstrate the benefit of using low-κ materials. The most obvious is that the overall rise time of the circuit decreases. In addition, the contribution of the FETs in the circuit to the rise time actually decreases with decreasing κ since the contribution of the devices (FETs) for $\kappa=2.4$ is below that of the devices at $\kappa=3.9$, shown in Fig. 2. Finally, the rate of change in the rise time as a function of $I_{d,\mathrm{sat}}$ decreases as κ decreases. The ramification is that the circuit will be more immune to variation in FET characteristics at lower κ values. This holds practical significance since the circuit will have increased immunity to FET-to-FET variation.

There are several different techniques under consideration for forming dielectrics with κ lower than that of SiO_2 interlayer dielectric (ILD). They can be classified into three general categories, spin-on, porous, and chemical vapor deposited materials. The spin-on materials include spin-on glass (SOG) in which dissolved siloxane-based precursors coalesce and react to form glassy films ($\kappa\sim2.5-4.0$),[7–9,13] and spin-on organic films ($\kappa\sim2.6-3.4$).[5,6] Composite materials, including porous films, combine the minimum dielectric constant of essentially free space with a matrix of silica or organic material. Aerogel and xerogel approaches use different film formation methods to achieve the porous film with a silica matrix ($\kappa\sim1.5-3.0$).[12,14] Organic-based dual-phase films have been developed using phase-separated materials, in which one phase is induced to create the matrix, and the other to create convex-surface shapes that can be removed (either through dissolution or vaporization) to leave free space ($\kappa\sim2.0-3.0$).[12] Chemical vapor deposition techniques cover a wide range of formation methods. One is the fluorination of SiO_2 films deposited by plasma-assisted CVD (PACVD) ($\kappa\sim3.5-4.0$).[1,2] This process is currently being employed in limited manufacturing; however, its modest κ improvement and potential for fluorine-induced reliability problems suggest that it will be a short-term solution. Thermal CVD of organic films called parylene use an aromatic precursor to deposit films directly onto the wafer via thermal cracking of a dimer source, and subsequent condensation and crosslinking ($\kappa\sim2.5-4.0$).[10] Another thermal CVD technique uses partially methylated silane/H_2O_2 condensates to form SiO_2-based films with $\kappa\sim2.5-4.0$.[11] Finally, there is PACVD of fluorinated organic films, which is the subject of this article ($\kappa\sim2.0-3.2$).[3,4]

Many different approaches have been applied to producing *a*-C:F,H films using plasmas, but the two most common types employed are capacitively coupled glow discharges [plasma enhanced CVD (PECVD)], and high-density plasmas (HDP). Capacitively coupled glow discharges typically operate in the range of 100 mTorr–20 Torr, with plasma density between 10^9 and $10^{11}\,\mathrm{cm}^{-3}$, and T_e between 3 and 10 eV. Variations of glow-discharge techniques include triode configurations to allow for independent substrate bias control, and power pulsing to control the degree of precursor dissociation.[21–23] High-density plasma systems have 100× higher plasma density and 1000× lower pressure than typical capacitively coupled discharges. Higher plasma densities permit higher dissociation rates of polyatomic molecules.[24] The benefit of such sources is that they provide simultaneous source and bias control at practical deposition rates. By independently controlling the substrate bias, it is possible to have gap fill and film property control. As will be shown, the properties of HDPCVD *a*-C:F,H films tend to be independent of the applied substrate bias. The decoupling of film properties from applied bias is desirable from a manufacturing point of view, since this allows process conditions to be independent of gap fill control.

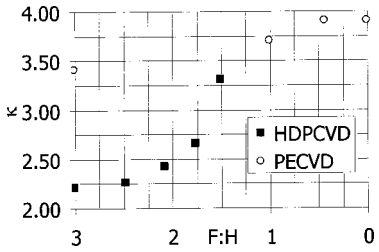

FIG. 3. κ as a function of gas mixture for HDPCVD and PECVD.

A variety of precursors have been tried for producing *a*-C:F,H films by both plasma generation techniques. The most common combinations are either single fluorine-containing compounds, or gas mixtures with at least one fluorine-containing precursor. Some of these precursors include CF_4, C_2F_6, C_2F_4, C_3F_6, CHF_3, C_4F_8, C_6F_6, C_6H_5F, HFPO, SF_6, NF_3, H_2, N_2, He, Ar, CH_4, C_2H_2, C_6H_6.[21–22,25–28]

III. RESULTS

Developing an understanding of a material created by plasma-assisted CVD requires knowledge of both the processes that lead to film formation and their physical properties. This understanding forms the basis for predicting how these films may behave in integrated circuits. Process-related results will focus on how process conditions such as plasma power, gas composition, and applied substrate bias affect optical and electrical properties of the films. Experiments of plasma power pulsing to control the degree of gas dissociation will be presented. Microstructural data related to film chemistry, adhesion, and thermal conductivity will then be presented. The third section results will be presented regarding integration of *a*-C:F,H films into the interconnect. This includes chemical and thermal stability studies, attempts to integrate the film into a metal/dielectric stack structure, and experiments to show how *a*-C:F,H may affect the performance and reliability of integrated circuits.

A. Process related

The gas mixture has the most profound influence on film properties like κ and C–C bonding configurations. Figure 3

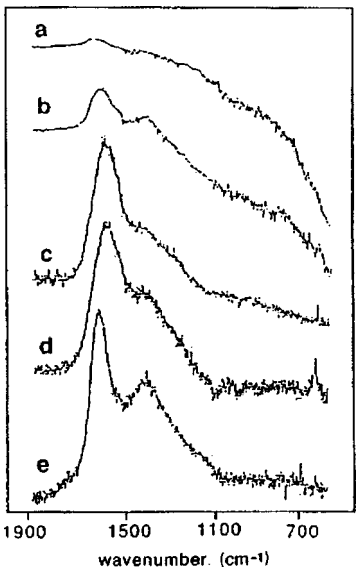

FIG. 4. Effect of applied substrate bias on PECVD *a*-C:F,H film properties (see Ref. 21). The applied voltages are (a) 0 V; (b) −50 V; (c) −100 V; (d) −150 V; (e) −200 V (courtesy of J. Vac. Sci. Technol. A).

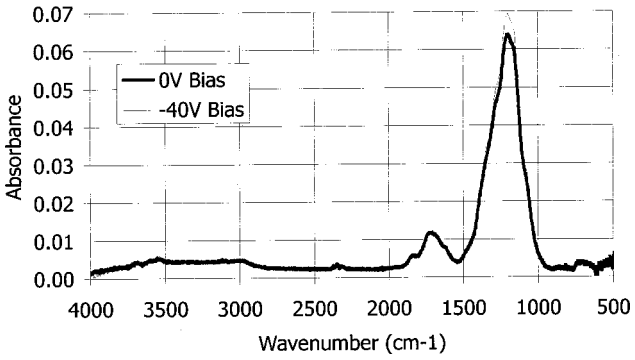

FIG. 5. Effect of applied substrate bias on the infrared spectrum of *a*-C:F,H films deposited by HDPCVD.

shows the effect of gas mixture on κ for HDPCVD and PECVD films.[3,27] For electron cyclotron resonance (ECR) HDPCVD films, the dielectric constant for the films decreases monotonically from 3.3 for an F:H ratio of 1.5 to 2.0 for an F:H ratio of 3.0.[3] For PECVD films using CF_4/CH_4 gas mixtures, on the other hand, κ only decreases from 3.8 with an F:H ratio of 0 down to 3.4 with an F:H ratio of 3.[27,28] For both classes of films, the trend is the same, as the F:H increases the dielectric constant decreases. Even though the parameter space of the data does not have much overlap, in general, the HDPCVD films have a lower dielectric constant.

Applied substrate bias for PECVD techniques is often used to modify film properties through ion-induced mechanisms. Raman spectroscopy has been used to study the effect of an applied substrate bias on the microstructure of *a*-C:F,H PECVD deposited films. Raman spectroscopy is sensitive to molecular vibrations that have no dipole like C–C bonds, making it ideal for detecting qualitative changes in sp^2 and sp^3C–C concentrations, the bonds that make up the *a*-C:F,H film backbone. In the study shown in Fig. 4, 8% C_2F_6 in H_2 was placed in a triode reactor (which provides for independent substrate bias control with respect to the plasma), and films were grown under substrate biases ranging from 0 to −200 V.[21] At low biases, the Raman spectrum revealed evidence of a film dominated by sp^2 bonds, implying that the films had a relatively low crosslink density and hence were more chain-like. At higher bias voltages around −100 to −150 V, the films had an increasingly higher fraction of sp^3 groups as in diamond-like carbon. This is clear evidence that the bias directly affects surface processes that contribute to film growth for PECVD films. For films grown in a parallel plate PECVD system it has been shown that for a constant CH_4/CF_4 gas mixture, changes in power produce changes in κ for films grown on the powered electrode, but not the grounded electrode.[28] Generally, in parallel plate systems, the self-biasing of the powered electrode varies in the same direction as the applied rf power. However, bias effects which are present for PECVD films, are absent for HPDCVD films. In HDPCVD deposition, κ is relatively constant over a wide range of applied bias voltages.[3] For example, for a given gas mixture, κ remains around 2.4 for applied rf biases up to −120 V. Infrared spectra of the films (see Fig. 5) also show no measurable change as a function of applied bias.[3]

In subtractive metal process flows where gap fill by the dielectric is required, it has been shown that HDPCVD processes need a substrate bias applied to produce complete filling. Unbiased HDPCVD *a*-C:F,H films tend to leave large voids. However, only a modest bias power (~30 W bias relative to 2000 W plasma power) produces excellent gap fill, especially for 2:1 aspect ratio gaps, relative to films with no applied rf bias.[29,30] One observation is that the peaked profile of deposited material on top of the metal feature has a steeper slope than that observed for Si-based films. This is related to differences in the angular dependence of the sputtering yields between carbon-based films and silicon-based films.[31] Since other film properties tend remain constant as a function of applied substrate bias, the implication is that controllable gap fill is possible with minimal impact on film performance. From a manufacturing perspective, this is advantageous since it provides for an extra degree of freedom for achieving gap fill with applied bias.

Plasmas create unique molecular intermediates for film deposition via various gas-phase impact mechanisms. The appropriate molecular mean free path, plasma volume, gas time constant, and plasma densities can create conditions that subject precursor molecules to multiple excitations, greatly expanding the number of species that contribute to film growth. Sometimes it is desirable to limit the number of species to control film composition. Power pulsing is one method by which the plasma chemistry can be tailored to control the composition of the deposited film. Pulsing the discharge lowers the mean number of excitation steps for a molecular fragment when the pulsing duty cycle is on the order of the molecular transit time through the plasma. Several groups have developed pulsed HDPCVD and PECVD techniques to deposit *a*-C:F, H films.[22,23,32,33] For example, Gleason and co-workers used hexafluoropropyleneoxide

(HFPO), which when thermally excited, decomposes producing the CF_2 radical which creates films consisting of predominantly networked CF_2 groups, or Teflon®-like films.[34] When HFPO is subjected to a continuous plasma, the resulting film shows a significant fraction of CF_3 and CF groups as measured by XPS.[32,33] Takahashi and co-workers have used ECR HDPCVD and simple fluorocarbon gases, with power pulsing at about 5%–15% duty cycle also produce films in which the CF_2 peak dominates XPS spectra.[22,23] It is generally believed that the CF_3 and CF radicals are formed by more extensive gas-phase dissociation of the precursor.[22] Shorter on-time pulses minimize the degree of precursor dissociation, leaving mostly CF_2 to form the film. Electron spin resonance measurements of these pulsed power low-duty cycle films show a 10× drop in dangling bonds compared with the continuous plasma deposition. This is an elegant example in which a PECVD process mimics a thermal CVD process but at lower temperatures.

Understanding the influences on plasma chemistry is the first step in developing a model of plasma-assisted CVD processes.[35,36] In the CH_xF_y plasma chemical system, it has been shown that the reactor walls (namely, temperature and surface composition), have a great influence on plasma composition. For example, an increase in the gas-phase CF_x density can be achieved by increasing the reactor wall temperature or by allowing the reactor wall to be covered with CF_x polymeric films.[35,37] In the case of reactor wall temperature, the concentration of CF_x fragments in the chamber was monitored using mass spectrometry of the plasma.[36] It was found that all CF_x species increased as a function of temperature; a 50 °C change in wall temperature lead to a 10× rise. This has the effect of shortening residence times for adsorbed species. The wall condition itself also influences adsorbed species residence times. For example, it has been found that the gas phase density of some CF_x species is dependent upon the buildup of *a*-C:F,H films on the reactor wall; as the film builds up, the steady state concentration of CF_x groups increases.[37] Changes not only in the elemental stoichiometry but also in the molecular structure of the injected gas mixture can affect the dissociation products. For example, H_2 dilution of perfluorinated compounds assists in the rate of their dissociation for HDP plasmas, whereas it actually inhibits dissociation in partially fluorinated compounds.[35]

B. Microstructure related

Carbon has multiple stable hybridizations, sp^3, sp^2, and *sp*, all of which are relatively immune to oxidation. Disordered allotropic carbon films vary from waxy polymeric materials, to graphitic complexes, to diamond-like networks. This means that the local environment for any atom in a carbon-based film has greater variation than for silicon-based films. It also implies that transformation of the local environment can be more complex. So paradoxically, while it is more difficult to define a picture of the microstructure for the film network, it is more important to try to understand it as it plays a larger role in defining film properties. Such understanding will allow exploitation of the microstructure to achieve desired performance. To this end, there has been a lot of activity to try to understand the microstructure of carbon-based networks and how to probe them. In the previous section, work has been presented relating the film properties to process conditions. This section examines work to elucidate details of the microstructure itself through XPS, thermal conductivity measurements, and adhesion studies.

TABLE I. Effect of fluorination on C 1*s* binding energy.

Binding energy (eV)	Functional group
285.1	–C– or –C–H
287.1	–C–CF
289.3	–CF–
291.5	$-CF_2-$
293.7	$-CF_3$

Infrared and Raman spectroscopy are complementary techniques that can be used to identify most molecular groups and interactions between them. Identification of the groups can be used to narrow the range of possible configurations present in the film, which can be used to gain a fundamental understanding of the microstructure. Because many potential vibrational modes can contribute to the spectral bands, the overall spectra of either infrared or Raman spectroscopy can be used to identify subtleties in the film structure that may be related to the film formation method. At the same time, the breadth and separation of the modes makes it difficult to decouple them from each other. Figure 5 is an infrared absorption spectrum of an *a*-C:F,H film deposited by an HDPCVD technique and a mixture of gases containing C, H, and F. The most intense band between 950 and 1550 cm^{-1} is related to C–F and C–F_2 groups of various vibrational modes. Single phonon-like processes may also exert a small influence in region.[38,39] Multivariate regression analysis of the band suggests that it may be composed of up to seven distinct subbands.[29] From around 1400 up to 1860 cm^{-1} are a series of groups that are assigned to C═C vinyl and phenyl groups.[40] Also, between 1680 and 1750 cm^{-1}, centered around 1720 cm^{-1}, there is a possibility of a band that might belong to C═O (carbonyl). A discussion about the existence of C═O groups in these films will be presented in the discussion section. When hydrogen is used during deposition there can also be a weaker band in the 2920–3000 cm^{-1} range due to alkane stretching modes.[40] A band in the region of 3650 cm^{-1} is sometimes seen as well; it is normally attributed to adsorbed H_2O or OH, and irreversibly disappears upon heating.[3]

In the C–F system, XPS data provide details about local bonding configurations between C and F, due to the very wide separation of C 1*s* peaks as a function of the degree of fluorination.[34] The wide peak separation is caused by the strong localization of the C 1*s* resulting from bound F. Table I shows the group assignments for the peaks as a function of the binding energy. The height of each peak is proportional to the fraction of C atoms with a given degree of fluorination

TABLE II. Thermal conductivities of thin films (see Ref. 42).

Material	Thermal conductivity (10^{-2} W cm^{-1} K^{-1})
a-SiO_2	1.4
DLC	0.3–1.0
a-Diamond	5.2–9.7
c-Diamond	2100
PMMA	0.2

near the surface of the sample, which allows for relative comparison of group concentration. XPS spectra of HDPCVD films deposited with and without applied bias show there is no real change in the film chemistry.[41] However, as will be shown later, the ability to chemically discern the degree of fluorination will prove to be helpful in relating deposition conditions to film properties that rely upon the coordination number of the amorphous film network.

One concern for integrated circuit reliability is heat dissipation, making it important that the materials in the interconnect have adequate thermal conductivity. Therefore any change in the materials in the interconnect must be viewed in terms of impact on thermal conductivity. Morath *et al.* have developed a relatively straightforward technique to measure the thermal conductivity of thin films.[42] They locally heat the film with a 200 fs laser pulse, and indirectly monitor the temperature decay rate from the spot by measuring the reflectivity change of the spot. They used this technique to measure the thermal conductivity of a series of *a*-C:H films and found that the thermal conductivity of *a*-C:H films has a roughly proportional correlation with fraction of sp^3C–C bonds.[42] Table II shows the thermal conductivities for a series of carbon-based materials. Diamond-like carbon (DLC) and *a*-diamond films both have a high fraction of sp^3C–C bonds, however DLC films are defined as having a higher degree of network-terminated bonds than found in *a*-diamond. (A network-terminated bond is one in which a multivalent atom bonds to a mono-valent atom.) Therefore, it is expected that DLC films have a lower thermal conductivity. The significance is that since *a*-diamond and DLC films can be deposited by PECVD techniques, thermal conductivity of *a*-C:F,H will depend heavily on the type of film formed. One note: it is well known that the mechanical rigidity and thermal conductivity of materials are related; diamond is very rigid and has high thermal conductivity, while polymeric materials do not. The same applies to carbon-containing thin films, in which films with more hydrogen are softer and have lower thermal conductivity.[43]

Adhesion of *a*-C:F,H films to other materials tends to be worse than that of other low-κ dielectrics. Much work has been done to improve adhesion to the point where *a*-C:F,H can be incorporated into most film stacks.[28,44,45] The most promising approach is to use deposited adhesion layers. It has been found that while HDPCVD *a*-C:F,H does not adhere to SiO_2, nor does SiO_2 adhere to *a*-C:F,H, some success can be achieved by using a 30 nm *a*-C:H film on either side of the *a*-C:F,H film.[28] A 30 nm film of *a*-C:H and a 30 nm silicon-rich sub-oxide layer improved adhesion even more.[44,45] XPS data shows that the appearance of Si–CC 1*s* band correlates with improved adhesion.[44] Other work shows that a SiC adhesion layer works with moderate success.[46]

C. Integration related

One of the major potential applications for these films is to use them as an ILD for high-performance integrated circuits. Such applications require that *a*-C:F,H is compatible with many other materials under adverse conditions without interfering with their formation or operation. Much effort has also been made to explore how *a*-C:F,H would affect other aspects of interconnect fabrication. This section presents a summary of the work to date to examine the stability of these films with respect to thermal cycling, and how chemically inert they are. Once films are deposited for ILD applications, it is important that they remain chemically stable, in that they neither react with other compounds nor release compounds that may react with other films. In addition, incorporation of *a*-C:F,H into the interconnect, and its impact on thermal performance of the circuit are presented.

Chemical stability is one of the most important concerns with respect to *a*-C:F,H films. It has generally been believed that *a*-C:F,H films might be chemically prone to oxidation, and a few papers have been devoted to this possibility. In work on plasma-polymerized films, the oxygen content on film surfaces by XPS, and bulk oxygen content were examined by secondary ion mass spectroscopy (SIMS) profiling of selected samples after aging.[47] PECVD films were grown at different power levels on polycarbonate substrates that were only between 200 and 400 Å, and found that immediately after deposition, a film deposited at 600 W had higher oxygen content than a film deposited at 100 W. It was also found that the film surface oxygen content increased when exposed to 65 °C, 85% relative humidity air for prolong periods of time. Another type of chemical stability concerns the mobility of fluorine in the film. Data from numerous sources show that films tend to lose fluorine as a function of heating, as shown by infrared spectra collected before and after heating.[3,48,49]

One concern about incorporating organic materials into integrated circuits is how they withstand the thermal cycling during subsequent processing steps. Many spin-on polymers suffer from degradation of electrical properties, volumetric shrinkage, adhesion failure, flow, and evolution of gases upon heating to 400 °C (the temperature of the final hydrogen drive-in for gate oxides). Therefore, one test required for organic films is to measure the thickness loss upon heating; a typical criterion is $<1\%$ thickness loss after 60 min at 400 °C. Most of the published work shows that neither PECVD nor HDPCVD produces better films with better thermal stability than the other.[3,4,48] It is possible to produce films with either great thickness loss, or virtually no thickness loss by both methods. It has also been reported that the film thickness can increase slightly upon heating in certain circumstances.[3,48] In the case in which film thickness increases with heating, it has been confirmed that the thickness

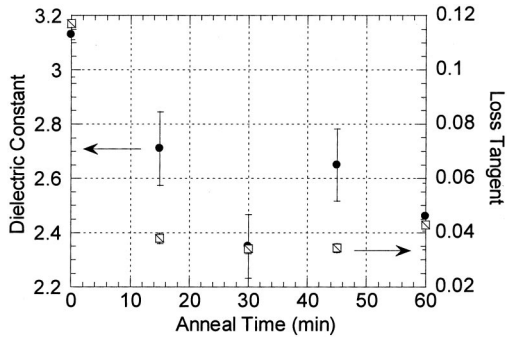

FIG. 6. κ and tan δ as a function of thermal heating duration at 400 °C in 4 Torr Ar.

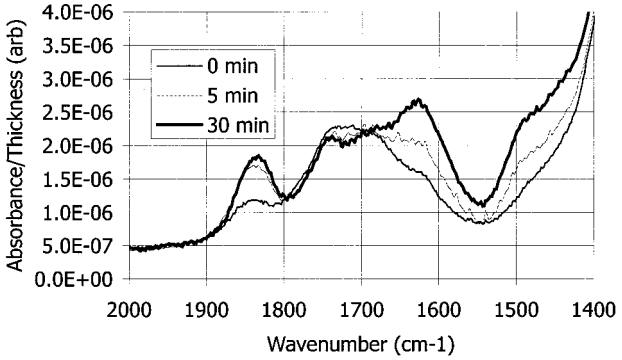

FIG. 8. Portion of infrared spectrum *a*-C:F,H films deposited by HDPCVD as a function of post-deposition thermal cycling duration at 400 °C in 4 Torr Ar.

increase is associated with a density decrease and that the films undergo other changes.[50] As the density decreases, there is a corresponding drop in both κ and tan δ (see Fig. 6). (Tan δ is a measure of the attenuation of the signal through the dielectric.) It has been shown that the density drop accounts for virtually all of the decrease in κ.[48,50] For example, when HDPCVD *a*-C:F,H films are heated they can exhibit a decrease in κ, tan δ, dangling bond density, film thickness, density, and the fluorine content (see Fig. 7). There are also notable changes in the infrared spectrum between 1400 and 1850 cm^{-1} (see Fig. 8).[3,49,50] The spectrum shifts upward with time around 1450, 1630, and 1830 cm^{-1}, and decreases slightly around 1730 cm^{-1}. All of the changes occur up to 30 min of heating at 400 °C, except for the band at 1830 cm^{-1}, which stabilizes in less than 5 min. This region of the infrared spectrum is associated with C═C vibrational modes.

Attempts to improve the thermal stability of *a*-C:F,H films typically rely on changing film composition. The most common method is to lower the ratio of F:H in the incoming gas feed.[3,4] It is possible to completely eliminate thickness loss by adjusting the F:H ratio, but it is usually at the expense of an increase in κ for as-deposited films. Another is to add N_2 to the feed gas for PECVD films.[51] It was found that for CF_4/CH_4 gas mixtures, adding N_2 reduced thickness loss from 40% to 0% at 300 °C for 60 min. These stable films contained about 12% nitrogen. This technique works at the expense of about a 15% increase in κ, but once again κ becomes stable with respect to heating.

Despite the uncertainties of chemical stability and difficulty in achieving adhesion, integration of *a*-C:F,H into a multilevel stack has been demonstrated.[30,52] Figure 9 shows a scanning electron microscopy (SEM) micrograph of a three-level metal structure with two layers of *a*-C:F,H films serving as the interlayer dielectric.[30] Most of the subtractive metal process flow modules are demonstrated: metal deposition, lithography, metal etch, low-*k* deposition, hardmask deposition, and hardmask chemical mechanical polishing (CMP).[30,45] One feature to note is that there is no CMP of the *a*-C:F,H dielectric. This leads to a nonplanar dielectric hardmask/low-κ interface between metal levels, although the overall dielectric is planar. A nonplanar interface will lead to more difficult control of the sidewall profile and erosion during via etch. However, since no one has revealed a successful planarization technique for *a*-C:F,H films, this is one of the few subtractive metal process flows that would work. Although the work of Endo *et al.* in Fig. 9 does not show vias through the *a*-C:F,H layer, a separate picture has been published showing an etched via through the material that has been filled with a CVD Al process [dimethyl-aluminum-hydride (DMAH) 180 °C] and a TiN barrier. Endo *et al.* have

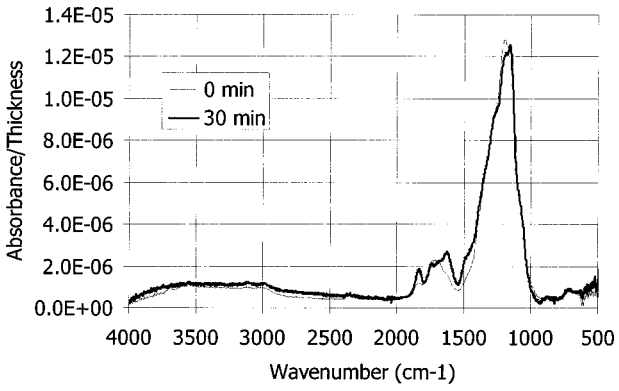

FIG. 7. Effect of thermal cycling for 30 min at 400 °C in 4 Torr Ar on infrared spectra for HDPCVD films.

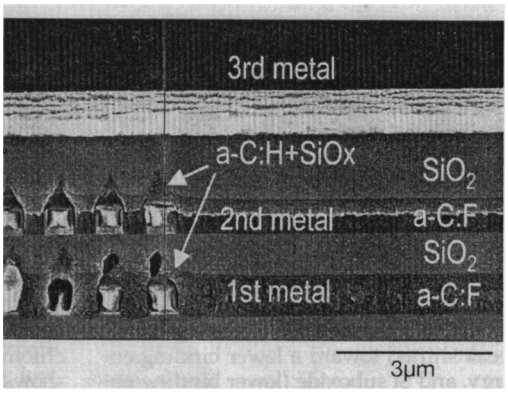

FIG. 9. Three level metal stack with two layers of a *a*-C:F,H film deposited by HDPCVD (see Ref. 30) (courtesy of the Materials Research Society).

shown that it is necessary to fabricate the entire interconnect structure below 300 °C, the thermal limit for their films.

With the ability to incorporate organic low-κ materials into simple interconnect structures, there has been some effort to test their effect on performance and reliability. The impact on capacitance by substituting *a*-C:F,H films for SiO_2 in the intralayer region of the interconnect has been studied.[30,45] It was shown that the capacitance does drop by about 50% when replacing SiO_2 with *a*-C:F,H. However, as mentioned previously, circuit speed enhancement does not scale entirely with reduction in κ. The effect of lowering the thermal conductivity of the interlayer dielectric was studied to see if there would be a significant degradation in electromigration lifetime.[53] A spin-on organic low-κ material with a thermal conductivity lower than that of SiO_2 was used in three different dielectric configurations: pure SiO_2, a SiO_2 layer between metal layers and an organic film between metal lines, and all organic material. It was found that there was no significant decrease in metal line lifetime for reasonable current densities any of the configurations. However, a very slight shortening of the lifetime was noted for the samples made entirely of polymer.

IV. DISCUSSION

While research into understanding *a*-C:F,H behavior has been somewhat scattered, it is possible to start developing a picture of how it forms, it structure, and the issues confronting the integration of them into integrated circuits. In terms of physical understanding, *a*-C:F,H provides a unique opportunity to glimpse at the connection between molecular features and macroscopic properties of thin films. By examining the average carbon coordination number within the film, it is possible to relate deposition parameters and film chemistry to macroscopic properties such as mechanical stiffness, thermal conductivity, stress, and perhaps thermal stability. The chemical stability of these films with respect to oxygen content, reaction with ambient oxygen sources, and mobility of fluorine will also be discussed. The effect of deposition and reactor conditions on plasma chemistry will be presented. The focus will be on the effect of the reactor design, wall condition, and gas dilution on precursor dissociation rates. It will be shown that the films may not be as reactive with environmental oxygen sources as sometimes assumed.

A. Process

Much of the published work has concentrated on the effect of deposition conditions such as gas precursor, gas flow, plasma generation technique, power and the like, on the deposited film properties. However, for *a*-C:F,H films, other aspects of the reactor play an influential role in the type of film produced. For example, the plasma etch community has studied analogous processes to understand etch selectivity, and sidewall film formation as a method of etch profile control.[54] What they have shown is that the composition of reactor wall surfaces and wall temperature variation can alter the radical mixture in the plasma by orders of magnitude. Several techniques have been employed to explore *a*-C:F,H properties. Raman and infrared spectroscopies can be used to identify local bonding groups in the films. XPS can quantify the relative concentrations of C with various degrees of fluorination. As will be shown later, these data can be used to predict film mechanical properties. Furthermore, this relation can be extended to other properties such as thermal stability and used to develop a model for the film properties as a function of deposition conditions. Finally, such a model can be helped in establishing connections between microscopic and macroscopic properties.

One of the most interesting observations is that applied substrate bias influences film properties for PECVD but not HDPCVD films. For PECVD, depositing on the powered electrode (where self-biasing can be a function of power), there is a change in dielectric constant not seen for the grounded electrode.[28] It has been shown that an applied bias can even limit material accumulation below certain processing pressures, while unbiased surfaces accumulated material at all pressures.[37] It is apparent that ion-activated processes dominate PECVD film growth under certain process regimes, through control of desorption rates and possibly decomposition processes. With an ionization fraction around 10^{-5}, the structure of the precursor gases may influence the film. Applying a bias to the substrate can result in the rearrangement of atoms on the surface, hence driving certain deposition reactions. In HDPCVD systems, on the other hand, applied substrate bias does not appreciably affect film properties. With very high ionization and dissociation rates for high-density plasmas, it is generally considered that molecular fragmentation is essentially complete. Therefore, the composition of the atomic flux density is what dominates film composition, so applying a substrate bias tends not to produce a net rearrangement of atoms.[24]

Power pulsing is another method of influencing the character of network forming bonds. The purpose of power pulsing is to enable plasma processes to approximate a thermal process but at lower process temperatures. It has been used to produce stable films that have an order of magnitude lower dangling bond density than films formed from continuous plasma deposition processes. The impact is to produce low-κ films that are less lossy. While it has not yet been demonstrated, there is no reason to expect that these films would suffer from significant degradation in thermal stability or mechanical properties with respect to continuous plasma films. The major drawback of power pulsing is that it could create plasma-induced damage in CMOS transistors. This is a problem that would not be easily minimized by process modification, as it would be difficult to remove spatial and temporal voltage gradients from the plasma of processing equipment.

The influence of reactor geometry and wall condition is rarely well characterized, although it often has been shown to affect process results. Experiments performed on *a*-C:F,H depositions show that these are no exception. Increasing wall temperature has been shown to increase CF_x concentrations in the discharge, since all radical concentrations scale at roughly the same rate, this causes a decrease in the desorp-

tion time.[36] This translates into a higher CF_x partial pressures, and can increase the film growth rate. For PECVD systems, this may lower the ion/neutral flux ratio at the surface which could alter film properties. The change in gas-phase radical equilibration time as a function of bias and pressure highlights two issues: (1) the wall condition controls the partial pressure of CF_x radicals, and (2) for PECVD, applied substrate bias controls film formation kinetics. Because the wall conditions may be continuously changing, the partial pressures of CF_x radicals do not remain proportional to one another, which shifts the reactant concentrations at the substrate surface. These shifts have the potential to form graded films. The ramification of changes to the surface state and wall temperature is that the deposition processes that control film properties may vary during the course of deposition and influence depositions from sample-to-sample by a reactor history effect. If these are not controlled or characterized, they will lead to inconsistencies in the results of process studies.

B. Microstructure

As with any material, it is desirable to understand the relationship between microstructural phenomena, and macroscopic properties in order to refine development. The C–F system in particular presents a unique opportunity to definitively make such connections. XPS will be used to predict the rigidity of the network and in turn this is related to film properties such as stiffness and thermal conductivity. In addition, density changes, electrical characterization, and infrared spectra will be used to develop a picture of the major contributors to the film dielectric constant.

The C–F chemical system provides a unique opportunity to probe the microstructure of *a*-C:F,H films. The ability to know the degree of fluorination of C atoms by XPS, enabled by the ~2 eV shift for each fluorine atom bound to a carbon atom (see Table I for the binding energies), allows one to determine the degree to which C atoms are constrained within the thin film network. Coordination number information is normally quite difficult to deduce due to the lack of readily available measurement techniques. However, with these data it is possible to start tying together microstructural features of *a*-C:F,H with macroscopic behavior like stiffness.

For C–F films, XPS spectra provide a complete description of the bonding of carbon atoms; therefore this can be used to determine the coordination number.[22] For example, the fracture mechanics of the films can be predicted by determining the coordination number (m), which is the average number of bonds that a carbon atom makes to other network-forming atoms.[22,55,56] The coordination number is theoretically calculated by estimating the limits of attainable networks of C atoms given all bonding configurations.[57] It has been shown that for $m>2.67$, the film is overconstrained, and fails with a brittle fracture, whereas for $m<2.15$, the film is underconstrained and fails with a good deal more plastic deformation.[56] Since fluorine is monovalent, it terminates the network where it bonds to carbon, therefore, the more fluorine the lower the coordination number. It has been

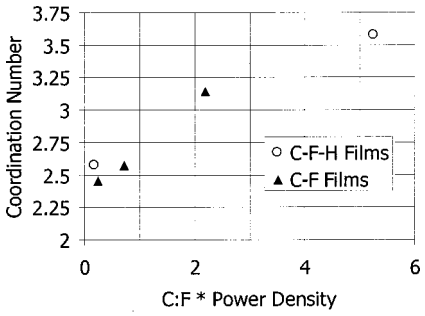

FIG. 10. Coordination number as a function of the product of C:F ratio and power density.

shown that XPS spectra of HFPO CVD and PECVD *a*-C:F,H films can be used to successfully correlate m to the fracture mechanism.[22] The estimate of the coordination number (shown in the following equation) is the sum of the product of the number of network bonds associated with each carbon group for each degree of fluorination and the fraction of those network bonds as shown by the XPS spectrum:

$$m = 0.01(\%CF_3) + 0.02(\%CF_2) + 0.03(\%CF) + 0.04(\%C\text{–}CF) + \%(C\text{–}C), \quad (1)$$

where m is the coordination number, and the CF_x terms are the fraction of each type of group that corresponds to the appropriate XPS binding energy peak.[22] One caveat to consider is that the calculation of m does not distinguish between sp^2 and sp^3 bonding. Even though this does not change the coordination number, the rigidity of the network will be lower with increasing presence of sp^2. However, since it has been shown that the fracture mechanics roughly correlate to m, then the concentration of sp^2 bonding is not high enough to greatly change the analysis.

Since the coordination number explains physical film properties, a model that describes m in terms of process parameters would be a powerful predictive tool. One way to relate the film properties with deposition conditions is to develop a simple empirical model that describes the data. Figure 10 is a plot of m calculated for several different films as a function of the product of the substrate power density and the C:F ratio of the gas mixture. The data in Fig. 10 come from five separate experiments (including parallel plate PECVD and HDPCVD sources, as well as CF_x and CF_xH_y gas mixtures), and all data points lie on a roughly straight line. In order to estimate the substrate power density, the substrate area was divided into either total plasma power was used for parallel plate configurations, or applied substrate bias power for nonparallel plate configurations. The fact that data from five separate sources all lie on the same line suggests that this relation accounts for relatively fundamental effects that control film growth. These effects are also relatively independent of many details of the process conditions; furthermore, the C:F ratio in the gas mixture, and the power density are the major factors.

The model works well for films in which the coordinating configuration for the network-terminating groups (atoms or

dangling bonds) are measurable. But one question that remains is why does this model also hold true for films grown with hydrogen in the gas mixture, and how do dangling bonds affect these film properties. For XPS, H and dangling bonds provide less than a 0.1 eV shift, compared with the fluorine-induced (~2.0 eV) shift of the C 1*s* binding energy making these difficult to resolve. Therefore, the concentration of hydrogen-terminated and dangling bonds must also be considered to see how they may perturb the analysis. In representative infrared spectra (see Figs. 5 and 8), the bands around 2900 cm^{-1} for C–H(s), and the 950–1550 cm^{-1} band for C–F(s) can be used to estimate the relative amount of hydrogen to fluorine in the film. The absorption intensity for C–H(s) varies from 0.45 for saturated hydrocarbons down to 0.08 in halogenated methyl groups, whereas C–F(s) has a value of 0.10.[40] Assuming that the band from 950 to 1550 cm^{-1} band is primarily related to C–F(s), then the area ratio of C–F(s) to C–H(s) is roughly around 300:1. Since F:H can be estimated from the ratio of the product of peak areas and the relative intensity terms, the ratio can be from 67 for the saturated hydrocarbon intensity to 375 for a halogenated methyl group. Given the sizable fraction of fluorine atoms in the film (upwards of 40%), which is likely to push the C–H(s) intensity towards halogenated methyl group strengths, the ratio is probably closer to 375.[29,48] In either case, it is clear that the H content of the films is likely to be quite low, and can be neglected. Dangling bond concentrations are also very low. From ESR data, the maximum dangling bond concentration is estimated at $10^{19}/cm^3$ in the as-deposited state, and for the thermally treated state concentration as low as $3 \times 10^{17}/cm^3$ dangling bonds account for only a few tenths of a percent of the network terminating sites,[49,58] and can also be neglected. The linearity of the C:F*power density product implies that the term is the dominant parameter in determining the coordination number. While the functionality of the relation is still open to interpretation, intuitively, the parameter can be thought of describing conditions favorable to crosslinking. Since both increasing the amount of carbon and energy available for film formation, the greater opportunity for atomic rearrangement to promote crosslinking.

What Fig. 10 shows is that the product of C:F and power density is proportionally related to the crosslinking of C atoms in the film. While it is generally accepted that increased ion bombardment of a growing film normally increases the crosslink density, and that power density is proportionally related to ion bombardment, then it follows that power density increases the crosslink density. What is also seen is that the presence of fluorine in the feedstock gas somehow inhibits crosslinking. While it is not clear what influence fluorine has on the mixture of the impinging flux at the film surface, it is possible that fluorine preferentially ties up bonding sites of the growing film. Crosslinking inhibition leads to lower film density and therefore lower κ. This would be an additional mechanism by which fluorine contributes to lowering κ (the other mechanism being electron localization). Also, it appears that fluorine inhibits the degree to which H is incorporated in the film, given that the apparent amount of H in the film is substantially lower than in the feedstock gas mixture. Incorporated hydrogen may be removed at the deposition surface, either through thermal desorption, abstraction reactions with fluorine, or insertion reactions by carbon containing groups.

Since network constraint describes the degree to which network forming atoms, i.e., C, can move within the film, it has been shown to govern mechanical properties such as stiffness.[22] It is likely, though, that it can also describe other macroscopic film properties such as thermal conductivity and mass thermal stability. With respect to mass thermal stability, certain mechanisms such as rates of desorption or dissociation of light molecular fragments are intimately related with the degree of crosslinking and therefore rely on the network constraint. For films in which these mechanisms dominate, the mass loss process, then it is possible to predict thermal stability from the C:F*power density product in much the same way it can be used to predict stiffness. Therefore, this relation provides a powerful tool to limit the range of acceptable process conditions, aids in the development of a physical understanding of film structure and formation, and provides a benchmark for optimizing the deposition process. Thermal conductivity of carbon allotropes is also likely to depend on network rigidity. As shown in Table II, polymeric films which have low *m* numbers also have much lower thermal conductivity than rigid networks such as diamond.

One interesting correlation in the heating of *a*-C:F,H is that tan δ decreases upon heating while peaks in the infrared spectra in the 1400–1850 cm^{-1} range generally increase. Tanδ is a measure of the sum of attenuation of an electric field as it passes through a dielectric, and represents interactions of the electric field with dangling bonds, dipoles, and low energy chemical bonds. Since the infrared spectrum in the 1400–1850 cm^{-1} range is associated with C═C bonds, the phenomena could be linked by the conversion of dangling bonds in neighboring sp^3 bonded carbon atoms into sp^2 bonds. This is supported by recent electron-spin resonance (ESR) work that demonstrates that there is a decrease of the dangling bond concentration upon heating.[49] It is reasonable to expect that heating the films could assist in microstructural rearrangement, and that the potential energy within the dangling bonds could overcome the energy barrier to convert sp^3 into sp^2 bonds. Other contributions to the increase of C═C concentration include the dissociation of C–F and C–H groups, and an associative desorption mechanism between neighboring monovalent atoms to create gaseous products. These sorts of reactions tend to increase the thermal stability of the amorphous network with respect to subsequent heating.

Infrared spectra can be quite useful in developing a picture of the molecular groups comprising a dielectric. However, making firm assignments of infrared features to specific molecular groups in amorphous films is not trivial due to the presence of disorder. While specific modes have been identified for C–F, C–C, C–O, and C–H groups of various combinations for pure compounds, it can be difficult to cleanly delineate them from one another.[40] Part of the issue is that

the local environment perturbs the wavefunction of the vibrating group and can shift its energy level tens of wavenumbers from its free-space position. In a crystalline solid, the shift is discrete due to the narrow range of local environment configurations, but in a disordered solid the shift can be spread between the free space and crystalline environments. Since the spacing of different modes may be narrower than the amount of shifting, overlap is inevitable. In the specific instance of carbon-based materials, the presence of sp^3, sp^2, and *sp* bonds, translates into many more possible bonding configurations, thus increases the number of vibrational bands possible. Finally, because of the disorder, symmetry constraints that would prohibit a net dipole moment for a given vibration are removed, thereby allowing normally infrared-inactive vibration to contribute to the spectrum. This symmetry breakdown provides low-level absorption not seen for other infrared systems with similar molecular groups.

C. Integration

Thermal stability of films is always important for CMOS circuit fabrication, regardless of the interconnect fabrication technique. One of the main reasons for this is that a forming gas anneal is required at the very end of the process flow to remove process-induced damage to the gate oxide and stabilize the interface. This forming gas anneal (4%–50% H_2 in N_2) is typically around 350–450 °C for 30–120 min. This is true even for the Cu-damascene process flow, in which all process temperatures except the forming gas anneal can be limited to 300 °C. For *a*-C:F,H films, it is also necessary that they are stable with respect to ambient oxygen sources, and have minimal fluorine mobility. Most carbon-based materials tend to have limited thermal stability, in the range of the forming gas anneal. In fact, it is not expected that organic films can meet the mass and thickness loss requirements of inorganic films like SiO_2. However, once the film is deposited, losses must be minimized to avoid unacceptably high structural strains. The above requirements lead most common thermal stability screening metrics that are applied for organic films to converge at $<1\%$ thickness loss after 30 min at 400 °C.

Most screening metrics do not account for mass loss, since as long as the film retains sufficient structural integrity, overall mass loss could be advantageous. However, certain issues, such as the fraction of potential outgassing material, the temperature-dependent rate of outgassing, and the forms in which fluorine may outgas, should be taken into account by any mass-loss metric. Even if fluorine is only released as an inert gas it does so after it is buried, which may result in a buildup of pressure to cause delamination and catastrophic failure. Therefore, the film must be stabilized in a single thermal cycle.

It is clear from the infrared data that fluorine diffuses from most of these films. Since atomic and molecular fluorine, and hydrogen fluoride (HF) are quite reactive, this leads to the question, if these are liberated in any significant quantity how will they affect integrated circuit reliability? It is widely known that HF and fluorine will corrode metal lines if they can penetrate through metal diffusion barriers. If they diffuse towards the gate regions, transistor performance might be degraded by creation of electrical defects at the gate interface and channel regions, by V_{th} shifts, and by lowering gate dielectric breakdown voltage. On the other hand, there are a variety of strategies that have been developed to prevent other contaminating elements (like Na, Cu, etc.) from reaching the substrate. For example, gettering and barrier films are routinely inserted into the interconnect. Diffusion barrier materials like transition metal nitrides are used to clad metal lines and may be effective diffusion barriers. Therefore, in order for the films to become realistic candidates for interlayer dielectrics (ILD), they either must be created such that mobile fluorine concentrations are minimized, or appropriate barriers must be inserted to prevent diffusion of fluorine to vulnerable structures and the films outgassed immediately before capping.

Several articles have suggested that *a*-C:F,H films are susceptible to post-deposition C═O formation. So far there has been no conclusive evidence to show that carbonyl (C═O) groups are an intrinsic feature of *a*-C:F,H films. It has been proposed that *a*-C:F,H films may be chemically prone to oxidation, but to date there is little firm data to support the contention. Most references to C═O groups point to infrared spectral bands that are in the same spectral region where carbonyl bands would exist. Work on plasma-polymerized films examined the oxygen content on film surfaces by XPS and attempted to examine bulk oxygen content by SIMS profiling after aging.[47]

Infrared spectroscopy is often used to identify the presence of C═O groups within thin films because of its distinct, narrow band in the 1720–1740 cm^{-1} range. However, using infrared spectra to identify a specific band in the region from 1450 to 1850 cm^{-1} for *a*-C:F,H films can be quite difficult since this is also the region for most C═C stretching vibrations.[40] The C═C bonds are among the bonds that form the amorphous network, and probably have a concentration on the order of $10^{22}\,cm^{-3}$. Given that the intensity of the C═O band is about 25× stronger than that of the C═C, the sensitivity for C═O detection is roughly $10^{20}\,cm^{-3}$. The carbonyl band can appear in the range of 1680–1780 cm^{-1} depending on whether the C═O is present as a ketone, ester, or carboxyl, and whether or not it is halogenated. Therefore, another possibility is that carbonyl-related spectral features are spread out over a relatively wide range. If the C═O is incorporated during film growth, then most of the aforementioned bond groups are possible, so it is not likely to have a distinct band. Changes that are seen in this region could also be attributed to conversion of dangling bonds and sp^3C–C bonds into C═C bonds.[3,49,50]

In the plasma-polymerization work on polycarbonate substrates, it was demonstrated that the film surface can oxidize over time.[47] However, it is not clear that the film bulk oxidized significantly over time, since XPS is a surface sensitive technique and SIMS profiling was performed only after aging. More importantly, the films deposited are so thin (200–400 Å), that it is unlikely that bulk SIMS data could be

extracted from the scans, and that the microstructure would not represent bulk films. Also, it is quite possible that oxygen is being incorporated during deposition. Depending on the configuration of the reactor, and deposition rate, it is possible for oxygen to be incorporated as a function of plasma power. At higher powers, the plasma volume may increase and liberate oxygen from newly exposed reactor surfaces. Also, the polycarbonate substrate itself contains a great deal of oxygen that may be incorporated during deposition, especially for such thin films. If the deposition rate is low, with a 10^{-5} Torr base pressure and a 10^{-2} Torr operating pressure, the partial pressure of oxygen might be high enough to have significant amounts of oxygen incorporated into the film. It is possible that the oxidation phenomenon that was reported is simply a surface mechanism and does not apply to the bulk. In any case, these films are likely to be too thin to be representative of integrated circuit applications, which typically use films for ILD that are at least 10×thicker.

There are several types of experiments that can be performed to answer some of these question with regard to post-deposition oxidation. *In situ* capping of the films with silicon nitride coupled with post-deposition monitoring, one way to determine whether or not there is a post-deposition oxidation effect. SIMS profiling of thick films deposited in oxygen-free environments (including the substrate) as a function of *ex situ* exposure time can also indicate if the films accumulate oxygen. However, care must be taken to differentiate between surface and bulk incorporation. Measuring the oxygen content as a function of substrate bias, gas flow rates, power, and deposition rate can also point to potential *in situ* sources.

D. Open integration issues

There are several issues that remain unresolved at this time. They mainly refer to adhesion, fluorine containment, and process flow. Before *a*-C:F,H can be considered for ILD applications, these issues need to be more or less resolved.

The two primary issues concerning adhesion are the applicability of the current process flows that utilize *a*-C:F,H, and the impact of adhesion promoting layers. While adequate adhesion of *a*-C:F,H has been demonstrated for one type of subtractive metal process, there are still some questions that need to be addressed for more conventional process flows. *a*-C:F,H can be inserted with adequate adhesion to form a multilayer interconnect structure in a CMP-free process flow. The adhesion layers that are most effective are bilayer films of silicon-rich oxide and *a*-C:H, and *a*-SiC films. In both cases, the films are higher κ materials, and may have higher tan δ. As these layers would lie adjacent to metal lines, they will have a disproportionately high influence on the composite κ, since they would lie in the path of the fringing electric fields. Work to reduce the adhesion layer thickness and positioning relative to metal lines will prove fruitful in improving performance.

One issue that has not been addressed is the effect of *a*-C:F,H outgassing on subsequent film deposition processes. If outgassing continues during later heating cycles, organic adsorption on deposition surfaces can interfere with film growth. It has been shown that for other organic materials continued outgassing can extinguish some metal CVD processes, and in other CVD processes lead to changes in metal morphology. It is also conceivable that physical vapor deposition (PVD) film growth can be disturbed. For example, since PVD Al grain growth can be interrupted by air exposure, organic material adsorption would most certainly have an analogous effect. If it is not possible to produce a film that stops outgassing, then it would be necessary to produce metal and barrier deposition processes that are not surface sensitive; however, this is a rather remote possibility.

A three-level metal process flow has been demonstrated for *a*-C:F,H films, showing it is possible to successfully integrate the material.[30] However, the process flow is quite different than other subtractive metal process flows. The non-planar dielectric topography over metal lines left by this process may prove difficult to work with for advanced via photolithography and etch. In addition, the entire process sequence was limited to 300 °C, presumably to not allow excessive thermal cycling for the material. Since forming gas anneals are required at the end of the process, this temperature restriction is too low. However, since adequate thickness stability has been demonstrated up to 400 °C for other *a*-C:F,H films, it is still possible to maintain more traditional process flows.[3,48] It will be easier to integrate *a*-C:F,H films into damascene process flows since CMP of the film would not be required. Metal CMP steps could make use of relatively thin inorganic hardmask layers, such as SiO_2, Si_3N_4, or SiC for the polish stop and adhesion layer. This would also probably require that the premetal dielectric not be *a*-C:F,H, since dielectric CMP planarization would be necessary. Regardless of process flow, certain other issues remain to be tackled. Via and trench etch process modules need to mature. It is likely that oxygen-based plasma chemistries will be used to etch *a*-C:F,H, but etch profile control may be difficult without hardmask erosion, as would resist stripping without *a*-C:F,H erosion or hardmask sputtering.

V. SUMMARY

In plasma deposition of *a*-C:F,H films, as the gas mixture goes towards fluorine-rich films, κ decreases but thermal stability tends to fall. One of the role of fluorine is to inhibit crosslinking. Applied substrate bias has been shown to affect film properties for PECVD films but does not affect those properties for HDPCVD films. However, it does improve gap-fill capabilities for HDPCVD deposited films. Power pulsing can be used to produce films that have lower dangling bond density and hence lower signal attenuation, but this may come at the cost of increased plasma induced damage. Wall temperature and composition have been shown to affect the plasma density of radicals, and are expected to affect the deposition rate accordingly. In addition, the nonlinear change in radicals as reactor walls ''season'' has the potential to create graded films.

While fluorine does lower κ through electron localization, it also contributes to a lower κ by lowering film density. In two reports, changes in κ correspond closely to changes in

density.[50,48] Thermal cycling has been shown to correspond to decreases in tan δ, dangling bond density, and increases in certain infrared bands in the 1400 to 1850 cm^{-1} range.[3,49,50] This can be explained by conversion of dangling bonds into sp^2 bonds, which improves film properties by making them less lossy. It has been shown how the average C coordination number may be measured by XPS and that this may be applied to predictions of the film properties such as mechanical stiffness, thermal conductivity, and mass-related thermal stability. It also has been shown that the product of C:F ratio and power density can be used as predictor of those film properties. Therefore, it is now possible to link microstructural features with macroscopic process conditions. Finally, conclusive data have yet to be published to show that C═O groups are an inherently intrinsic component of *a*-C:F,H films. Oxygen incorporated into these films is more likely to be only part of the film surface.

Most thermal stability specifications only consider volumetric losses at 400 °C and studies to date show that *a*-C:F,H films can be produced to meet those specifications. However, all of these films lose fluorine at least during the initial thermal cycle. This fluorine loss must be controlled through some sort of barrier if *a*-C:F,H films are to be considered serious ILD candidates. It has been shown for these films that interconnect capacitance is lowered in proportion to the κ value, and that from an electromigration standpoint, the potential for problems due to thermal conductivity is minimal. Adhesion of the bare film has been shown to be problematic, but it may be overcome using the appropriate adhesion layers. The inability to planarize *a*-C:F,H using CMP is an issue for conventional subtractive metal process flows; however, a nontraditional flow can work as has been demonstrated. For damascene process flows, encapsulating *a*-C:F,H with inorganic hardmask films produces on ILD with fewer problems. As described previously, encasing the interconnect metal in silicon oxide or polymeric material make very little difference to the electromigration lifetime. The significance is that substitution in the intralayer regions of one poor thermal conductor in the intralayer regions for another does not significantly alter the heat flow. Therefore thermal conduction is likely to be a manageable issue.

In summary, it has been shown that thermally stable materials of $\kappa \sim 2.3$ have been produced and incorporated into multilayer interconnect structures using existing manufacturing equipment. The κ of the films appears to be governed by fluorine-controlled density and electron localization, and tan δ can be minimized by removing dangling bonds through thermal annealing. Problems with fluorine migration have to be controlled in order to use this material, so any potential process flow using *a*-C:F,H films will likely differ substantially from current process flows. Finally, it was shown that XPS data can be used to has demonstrate a connection between microstructural features and macroscopic film properties. The use of this data along with a simple metric based on process parameters produces a predictive model for film properties as well as providing an initial description of *a*-C:F,H film formation.

ACKNOWLEDGMENTS

The author would like to thank Francoise Mertz, Gerrit Kooi, Karen Seaward, and Gary Ray of the Hewlett–Packard Company for their contributions. The author would especially like to thank Sam Nakagawa of the Hewlett–Packard Company for his assistance in modeling the effect of changes in κ on integrated circuit performance.

[1]T. Usami, H. Ishikawa, and H. Gomi, Mater. Res. Soc. Symp. Proc. **476**, 69 (1997).
[2]C. S. Pai *et al.*, Proceedings of the International Interconnect Technology Conference, Piscataway, NJ, 1998, p. 39.
[3]J. Theil, F. Mertz, M. Yairi, K. Seaward, and G. Ray, Mater. Res. Soc. Symp. Proc. **476**, 31 (1997).
[4]K. Endo and T. Tatsumi, Appl. Phys. Lett. **68**, 2864 (1996).
[5]H. Y. Tong *et al.*, Mater. Res. Soc. Symp. Proc. **476**, 75 (1997).
[6]J. Pellerin, R. Fox, and H.-M. Ho, Mater. Res. Soc. Symp. Proc. **476**, 113 (1997).
[7]J. N. Bremmer, Y. Liu, K. G. Gruszynski, and F. C. Dall, Mater. Res. Soc. Symp. Proc. **476**, 37 (1997).
[8]L. K. Figge, V. Flores, and S. P. Lefferts, Proceedings of the International Interconnect Technology Conference, Piscataway, NJ, 1998, p. 286.
[9]R. N. Vrtis, K. A. Heap, W. F. Burgoyne, and L. M. Robeson, Mater. Res. Soc. Symp. Proc. **443**, 171 (1997).
[10]M. A. Plano, D. Kumar, and T. J. Cleary, Mater. Res. Soc. Symp. Proc. **476**, 213 (1997).
[11]S. McClatchie, K. Beekmann, A. Kiermasz, and C. Dobson, Diel. for ULSI Multilevel Interconnection Conference Proceeding, Pittsburgh, PA, 1997, p. 34.
[12]K. R. Carter, Mater. Res. Soc. Symp. Proc. **476**, 87 (1997).
[13]K. Usami, S. Sugahara, K. Sumimura, and M. Matsumura, Mater. Res. Soc. Symp. Proc. **511**, 27 (1998).
[14]C. Jin, S. List, and E. Zielinski, Mater. Res. Soc. Symp. Proc. **511**, 213 (1998).
[15]O. S. Nakagawa, D. M. Sylvester, J. G. McBride, and S.-Y. Oh, Hewlett-Packard J. **49**, 39 (1998).
[16]T. Sakurai, IEEE Trans. Electron Devices **40**, 118 (1993).
[17]B. El-Kareh and R. J. Bombard, *Introduction to VLSI Silicon Development* (Kluwer, Boston, 1986), p. 522.
[18]E. D. Fabricius, *Introduction to VLSI Design* (McGraw–Hill, New York, 1990), p. 184.
[19]O. S. Nakagawa, K. Rahmat, S.-Y. Oh, G. Ray, and R. Kumar, ULSI XI Conference Proceeding, Pittsburgh, PA, 1996, p. 129.
[20]N. Rohrer *et al.*, Int. Solid State Circuit Conference, Piscataway, NJ, 1998, p. 240.
[21]R. D'Agostino, R. Lamendola, P. Favia, and A. J. Giquel, J. Vac. Sci. Technol. A **12**, 308 (1994).
[22]S. J. Limb, K. K. Gleason, D. J. Edell, and E. F. Gleason, J. Vac. Sci. Technol. A **15**, 1814 (1997).
[23]K. Takahashi, M. Hori, S. Kishimoto, and T. Goto, Jpn. J. Appl. Phys., Part 1 **33**, 4181 (1994).
[24]K. L. Seaward, J. E. Turner, K. Nauka, and A. M. E. Nel, J. Vac. Sci. Technol. B **13**, 118 (1995).
[25]S. Taheishi, H. Kudo, R. Shinohara, M. Hoshino, S. Fukuyama, J. Yamaguchi, and M. Yamada, Diel. for ULSI Multilevel Interconnection Conference Proceeding, Pittsburgh, PA, 1996, p. 71.
[26]S. F. Durrant, E. C. Rangel, N. C. da Cruz, S. G. C. Castro, and M. A. Bica de Moraes, Surf. Cont. Technol. **86**, 443 (1996).
[27]K. Endo and T. Tatsumi, Mater. Res. Soc. Symp. Proc. **381**, 249 (1995).
[28]K. Endo and T. Tatsumi, J. Appl. Phys. **78**, 1370 (1995).
[29]J. Theil (unpublished data, 1996).
[30]K. Endo, MRS Bull. **22**, 55 (1997).
[31]J. S. Logan, M. J. Hait, H. C. Jones, G. R. Firth, and D. B. Thompson, J. Vac. Sci. Technol. A **7**, 1392 (1989).
[32]C. B. LaBelle, S. J. Limb, K. K. Gleason, and J. A. Burns, Mater. Res. Soc. Symp. Proc. **443**, 189 (1997).
[33]K. Takahashi, M. Hori, S. Kishimoto, and T. Goto, Jpn. J. Appl. Phys., Part 1 **33**, 4181 (1994).
[34]S. J. Limb, C. B. Labelle, K. K. Gleason, D. J. Edell, and E. F. Gleason, Appl. Phys. Lett. **68**, 2810 (1996).

[35]K. Miyata, M. Hori, and T. Goto, J. Vac. Sci. Technol. A **14**, 2343 (1996).
[36]H. Sugai, K. Nakamura, Y. Hikosaka, and M. Nakamura, J. Vac. Sci. Technol. A **13**, 887 (1995).
[37]K. Maruyama and T. Goto, J. Phys. D: Appl. Phys. **28**, 884 (1995).
[38]K. McNamara Rutledge and K. K. Gleason, Chem. Vap. Deposition **2**, 37 (1996).
[39]K. M. McNamara, B. E. Williams, K. K. Gleason, and B. E. Scruggs, J. Appl. Phys. **76**, 2466 (1994).
[40]A. S. Wexler, Appl. Spectrosc. Rev. **1**, 29 (1967).
[41]K. Endo and T. Tatsumi, NEC Res. Dev. **38**, 287 (1997).
[42]C. J. Morath, H. J. Maris, J. J. Cuomo, D. L. Pappas, A. Grill, V. V. Patel, J. P. Doyle, and K. L. Saenger, J. Appl. Phys. **76**, 2636 (1997).
[43]S. Kaplan, F. Jansen, and M. Machonkin, Appl. Phys. Lett. **47**, 750 (1985).
[44]K. Endo, T. Tatsumi, and Y. Matsubara, Appl. Phys. Lett. **70**, 1078 (1997).
[45]Y. Matsubara, K. Endo, T. Tatsumi, H. Ueno, K. Sugai, and T. Horiuchi, International Electron Device Meeting, Piscataway, NJ, 1996, p. 369.
[46]T. W. Mountsier and J. A. Samuels, Proceedings of the International Interconnect Technology Conference, Piscataway, NJ, 1998, p. 280.
[47]M. Horie, J. Vac. Sci. Technol. A **13**, 2490 (1995).
[48]A. Grill, V. Patel, S. A. Cohen, D. C. Edelstein, J. R. Paraszczak, and C. Jahnes, Adv. Metall. and Intercon. Sys. for ULSI Appl. 1996, MRS Conf. Proc. XII, Pittsburgh, PA, 1997, Vol. B12, p. 417.
[49]H. Yokomichi, T. Hayashi, and A. Masuda, Appl. Phys. Lett. **72**, 2704 (1998).
[50]J. A. Theil, G. Kooi, F. Mertz, G. Ray, and K. Seaward, Proceedings of the International Interconnect Technology Conference, 1998, p. 128.
[51]K. Endo and T. Tatsumi, Appl. Phys. Lett. **68**, 3656 (1996).
[52]Y. Matsubara, K. Endo, T. Tatsumi, H. Ueno, K. Sugai, and T. Horiuchi, Int. Electron Device Meeting Proceeding, 1996, p. 369.
[53]S.-P. Jeng *et al.*, ULSI XI Conference Proceeding, 1996, p. 15.
[54]G. S. Oehrlein, Y. Zhang, D. Vender, and M. Haverlag, J. Vac. Sci. Technol. A **12**, 323 (1994).
[55]J. Phillips, J. Non-Cryst. Solids **34**, 153 (1979).
[56]G. H. Dohler, R. Dandoloff, and H. Bilz, J. Non-Cryst. Solids **42**, 87 (1980).
[57]J. C. Angus and F. Jansen, J. Vac. Sci. Technol. A **6**, 1778 (1988).
[58]C. B. Labelle, S. J. Limb, and K. K. Gleason, J. Appl. Phys. **82**, 1784 (1997).